MoS_2 nanosheets via electrochemical lithium-ion intercalation under ambient conditions

Mohamed El Garah,[1‡] Simone Bertolazzi,[1‡] Stefano Ippolito,[1‡] Matilde Eredia,[1] Iwona Janica,[2] Georgian Melinte,[3] Ovidiu Ersen,[3] Giovanni Marletta,[4] Artur Ciesielski[1*] and Paolo Samorì[1*]

[1]University of Strasbourg, CNRS, ISIS UMR 7006, 8 Allée Gaspard Monge, 67000 Strasbourg, France.

E-mail: samori@unistra.fr , ciesielski@unistra.fr

[2]Centre for Advanced Technologies, Adam Mickiewicz University, Umultowska 89c, 61-614 Poznań, Poland.

[3]University of Strasbourg, CNRS, IPCMS UMR 7504, 23 rue du Loess, 67034 Strasbourg, France.

[4]Laboratory for Molecular Surfaces and Nanotechnology (LAMSUN), Department of Chemical Science, University of Catania and CSGI, Viale A. Doria 6, 95125 Catania, Italy.

Abstract

Two-dimensional (2D) transition metal dichalcogenides (TMDs) are continuously attracting attention for both fundamental studies and technological applications. The physical and chemical properties of ultrathin TMD sheets are extraordinarily different from those of the corresponding bulk materials and for this reason their production is a stimulating topic, especially when the preparation method enables to obtain a remarkable yield of nanosheets with large area and high quality. Herein, we present a fast (<1 hour) electrochemical exfoliation of molybdenum disulfide (MoS_2) *via* lithium-ion intercalation, by using a solution of lithium chloride in dimethyl sulfoxide (DMSO). Unlike the conventional intercalation methods based on dangerous organolithium compounds, our approach leads to the possibility to obtain mono-, bi- and tri-layer thick MoS_2 nanosheets with a large fraction of the semiconducting 2H phase (~60%), as estimated by X-ray photoelectron spectroscopy (XPS). The electrical properties of the exfoliated material were investigated through the fabrication and characterization of back-gated field-effect transistors (FETs) based on individual MoS_2 nanosheets. As-fabricated devices displayed unipolar semiconducting behavior (*n*-type) with field-effect mobility $\mu_{FE} \leq 10^{-3}$ cm^2 V^{-1} s^{-1} and switching ratio $I_{on}/I_{off} \leq 10$, likely limited by 1T/2H polymorphism and defects (e.g. sulfur vacancies) induced during the intercalation/exfoliation process. A significant enhancement of the electrical performances could be achieved through a combination of vacuum annealing (150 °C) and sulfur-vacancy healing with vapors of short-chain alkanethiols, resulting in μ_{FE} up to 2×10^{-2} cm^2 V^{-1} s^{-1} and $I_{on}/I_{off} \approx 100$. Our results pave the way towards the fast preparation ─ under ambient conditions ─ of semiconducting MoS_2 nanosheets, suitable for application in low cost (opto-)electronic devices.

Keywords: Electrochemical exfoliation, lithium ions, molybdenum disulfide, field-effect transistor

1. Introduction

During the last years, transition metal dichalcogenides (TMDs) became the subject of a major research endeavor due to their unique physical and chemical properties [1-5]. The family of TMDs comprises materials with electronic properties spanning from insulating to semiconducting and metallic. Such a breadth of properties was fundamental to the development of various technologically relevant studies and processes to exploit in different potential applications, such as energy conversion and storage [6-8], electronics [9-11] and sensing [12, 13]. TMDs exhibit strong in-plane covalent bonds and weak van der Waals interactions between adjacent layers. As in the case of graphite, van der Waals forces between the layers of TMDs are weak enough to allow their exfoliation by exploiting external stimuli. Moreover, single-layer nanosheets of TMDs possess different properties from those of their bulk counterparts. By considering these various advantages, many approaches are being explored to exfoliate TMDs into single- or few-layer thick sheets. Their exfoliation into isolated layers has been achieved using different processes such as mechanical exfoliation [14], sonication and dispersion in liquid media [15-19] and electrolysis [20-22]. In particular, the electrochemical exfoliation is more advantageous compared to other *top-down* methods since it allows the formation of nanoflakes in a short time (ranging from a few minutes to a few hours) and takes place under ambient conditions (by exploiting different electrolytes), providing thin layered nanosheets with large area and high quality [23].

Among the TMDs, molybdenum disulfide (MoS_2) is the most investigated material due to its abundance in nature and its widespread use as a lubricant [24, 25]. The electrochemical exfoliation of a bulk MoS_2 crystal typically leads to the formation of isolated nanoflakes with two distinct crystal structures, i.e. the semiconducting (2H) and metallic (1T) phases [26]. More specifically, chemical exfoliation *via* lithium-ion intercalation leads to the formation of electron-rich nanosheets, characterized by a large fraction ─ between 60 and 70% ─ of 1T (or distorted 1T′) polytype [27]. Single-phase semiconducting nanoflakes have been obtained by means of post-exfoliation processes, such as thermal annealing [28], laser irradiation [18] and exposure to microwaves [29]. Exploiting the electrochemical intercalation process, Ejigu and co-workers [30] recently reported the exfoliation of a

MoS_2 pellet by using lithium perchlorate ($LiClO_4$) dissolved in a mixture of ethylene carbonate (EC) and dimethyl carbonate (DMC): the experiments were carried out under inert atmosphere (N_2), lasted for ca. 2 hours and resulted in a percentage of semiconducting 2H phase around 40%.

Here, we report on a simple and low-cost electrochemical intercalation process of MoS_2 crystals *via* DMSO-solvated lithium-ion, where lithium chloride (LiCl) is used as source of lithium ions. The use of DMSO leads to the formation of Li^+-DMSO adducts that can penetrate in between MoS_2 layers and increasing the interfacial spacing. Its effect is proven by the large expansion of MoS_2 crystal after the intercalation process. The latter is performed under ambient conditions, without any additives, and leads to the formation of mono- and few-layer thick nanosheets with ~60% of 2H phase. Our approach avoids the use of dangerous and explosive n-butyllithium [31-33] or expensive lithium foils [21]. The entire process can be easily performed under ambient conditions in less than 1 hour. We also explore the electronic properties of the exfoliated nanosheets through the fabrication and characterization of back-gated field-effect transistors (FETs) built on individual MoS_2 nanoflakes (2-4 layers thick) by means of electron-beam nanolithography. As-fabricated FETs display a unipolar *n*-type behavior similar to that of semiconducting MoS_2 nanosheets obtained by micromechanical cleavage (i.e. scotch-tape method). We further show that the electrical characteristics of the FETs can be significantly improved through a combination of thermal annealing (150 °C) under vacuum conditions (5×10^{-8} mbar) and vapor exposure to short-chain alkanethiols; a technique that we recently developed for healing sulfur vacancies generated by low-energy ion irradiation [34]. Such approach allows the increasing of μ_{FE} up to 2×10^{-2} $cm^2 V^{-1} s^{-1}$ and enables I_{on}/I_{off} ratio ≈ 100. In particular, upon exposure of the devices to vapors of short thiolated molecules (i.e. butanethiol), μ_{FE} increases by over a factor 3, suggesting that sulfur vacancies are an abundant type of defects in nanosheets exfoliated *via* DMSO-solvated lithium-ion intercalation. Furthermore, the large discrepancy between the aforementioned μ_{FE} and I_{on}/I_{off} values and those of state-of-the-art devices − based on high-quality MoS_2 nanosheets obtained by mechanical exfoliation via scotch tape peeling − highlights the presence of a more complex/detrimental disorder, which requires to be minimized towards practical (opto-)electronic applications. At this stage, our novel approach enables an easy and fast preparation of a large fraction

of 2H MoS_2 nanosheets under ambient conditions. Moreover, it casts the basis for more comprehensive studies of the effects of exfoliation-induced disorder on the charge-transport properties of ultrathin MoS_2 FETs.

2. Methods

2.1 Materials

MoS_2 crystals were obtained from SPI Supplies. Lithium chloride, dimethyl sulfoxide (DMSO) (≥99%) and 1-butanethiol were purchased from Sigma-Aldrich and were used as received.

2.2 MoS_2 electrochemical exfoliation

A piece of MoS_2 crystal (7 × 4 mm, 1 mm thick) and a Pt wire were used as working and counter electrodes, respectively. Some reported works on the lithium-ion electrochemical methods showed an optimal potential in DMSO, EC/DMC or other around 4─5 V [30, 35]. By using a two electrodes cell and applying a cathode-potential of 5 V, the expansion and intercalation process of MoS_2 bulk crystal is achieved during a time of 45 minutes using, as electrolyte and source of lithium ions, a 1 M solution of LiCl in DMSO (see Fig. S2 in Supplementary data). Then, the intercalated material was washed several times with acetone, filtrated, dispersed in a mixture DI H_2O (70%)/ethanol (30%) and finally exposed to sonication step (25 min). The dispersion was centrifuged at 4500 rpm for 30 minutes, in order to separate the thick unexfoliated materials, and then the supernatant was collected and used for the preparation of the samples. The concentration is estimated by taking 1 mL of the resulted solution, heating it up to evaporate the solvent and weighing the collected powder: the estimated average concentration of the dispersion is ~10 mg/mL.

2.3 Characterization

Dispersed MoS_2 nanoflakes were transferred in a 10 mm path length quartz cuvette and analyzed by means of UV-vis-IR absorption spectroscopy using a Jasco V670.

HR-TEM characterization was performed using a FEI Tecnai F20 TEM equipped with a Schottky emitter (200 keV). The samples were prepared by drop casting on a holey carbon-copper grid, followed by solvent evaporation.

XPS experiments were carried out with a Thermo Scientific K-Alpha X-ray photoelectron spectrometer equipped with an aluminum X-ray source (energy 1,486.6 eV) at a base pressure of 10^{-8}-10^{-9} mbar. The X-ray beam spot size was ~400 μm. All spectra have been referenced to C1s adventitious carbon at 284.8 eV. The peak fitting was performed with constraints on the full width half maximum (FWHM) and the peak-area ratio of the spin-orbit components.

Raman spectra were acquired at room temperature with a Renishaw InVia spectrometer equipped with a 532 nm laser. The measurements were carried out in ambient air using a 100× lens objective (numerical aperture NA = 0.85) providing a beam spot size of ~700 nm. The excitation power was kept below 1 mW to avoid local heating and damage effects.

Back-gated FETs were fabricated on thermally-oxidized heavily n-doped silicon substrates ($\rho_{Si} \approx$ 0.001 Ω·cm, $t_{ox} \approx$ 290 nm) by means of e-beam nanolithography, thermal evaporation of Au (90 nm) and lift-off. Electrical measurements were carried out under inert atmosphere (N_2-filled glovebox) with source-measurement units from Keithley (model 2636A).

3. Results and discussion

3.1 Structural properties of DMSO-solvated lithium-ion intercalated MoS_2 nanosheets

Lithium compounds have been widely used to intercalate and exfoliate layered materials into 2D nanoflakes. When DMSO is employed as the electrolyte, lithium ions can coordinate with the solvent to form DMSO-solvated lithium-ion complexes $(Li^+\text{-DMSO})_x$ [36]. Westphal and Pliego have theoretically demonstrated that lithium tends to connect with four DMSO molecules [37]. $Li^+(DMSO)_x$ species can penetrate in between the MoS_2 layers causing an increasing of the interfacial spacing. As displayed in the Fig. S1, in the supplementary data, a significant expansion of the crystal can be clearly seen which confirm the intercalation process. LiCl was dissolved in DMSO (1 mol/L solution) and served as electrolyte and source of lithium ions, while a bulk crystal of MoS_2 and a platinum wire

were used as working and counter electrode, respectively. The expanded material was then dispersed in a water/ethanol mixture and sonicated for 25 minutes to obtain mono- and few-layer thick MoS_2 nanosheets.

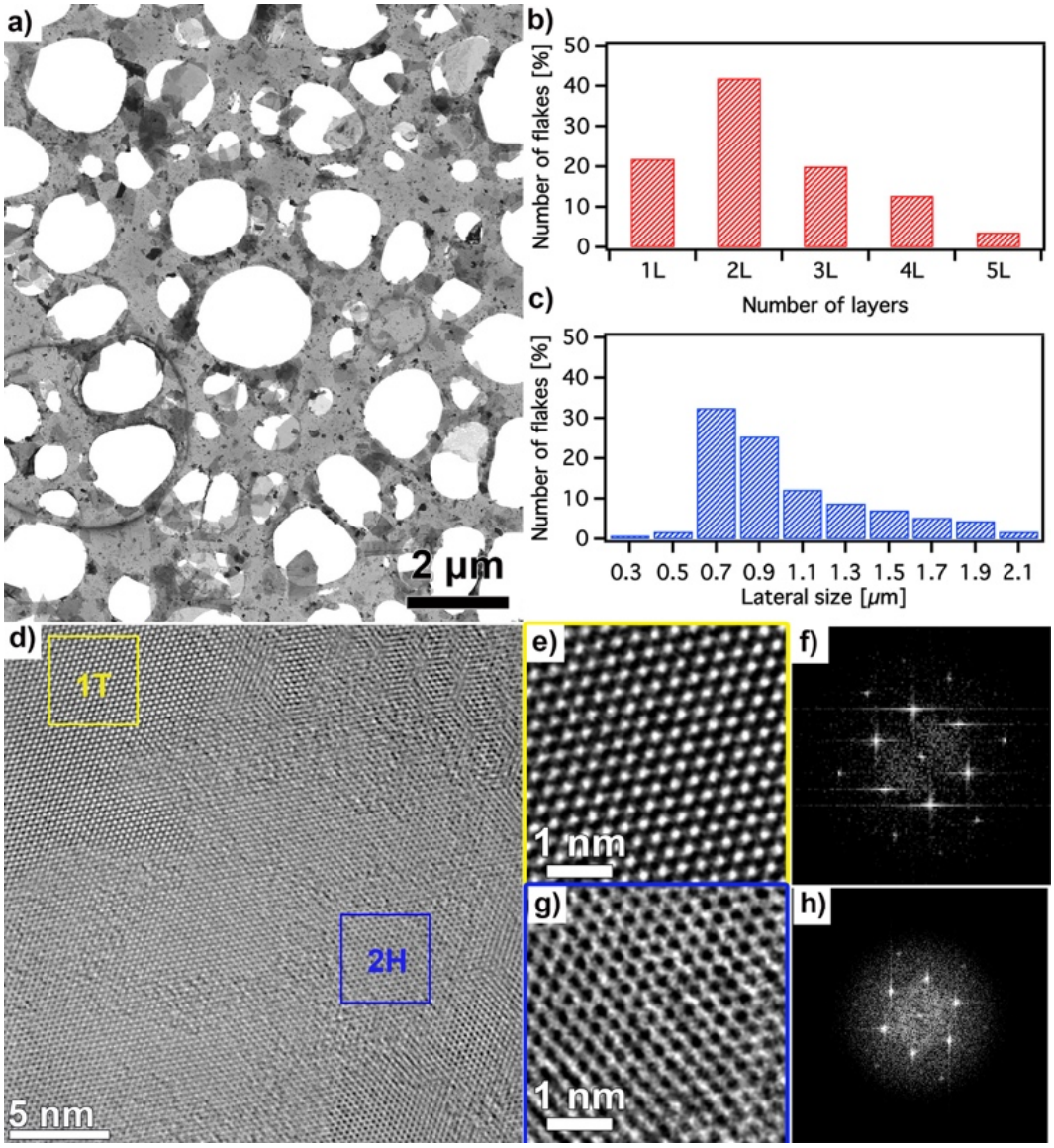

Fig. 1. (a) STEM image of MoS_2 nanosheets exfoliated via lithium-ion intercalation in DMSO and deposited onto a holey carbon grid. (b) Thickness distribution obtained from STEM measurements on 60 different nanoflakes. (c) Lateral-size distribution based on data from 150 different nanoflakes. (d) HR-TEM image showing the presence of two distinct crystalline phases. (e) Zoom-in image of the 1T region marked in yellow and (f) its corresponding diffraction pattern. (g) Zoom-in image of the 2H region marked in blue and (h) its corresponding diffraction pattern.

Fig. 1 displays scanning transmission electron microscopy (STEM) images of the exfoliated MoS_2 nanosheets with different lateral sizes and thicknesses. To give an estimation of the size and the

thickness of resulted nanosheets, we performed STEM and HR-TEM statistical studies on 150 and 60 nanoflakes produced by different batches, respectively. The analysis revealed the presence of a large amount of mono-, bi- and tri-layer thick MoS_2 nanoflakes with an average lateral size of ~0.8 μm. HR-TEM images (Fig. 1d, e and g) reveal the existence of two crystal phases within individual MoS_2 nanosheets, i.e. 1T (highlighted in yellow) and 2H (highlighted in blue), with characteristic diffraction patterns (Fig. 1f and h, respectively)

3.2 Spectroscopic investigation

The optical properties of the exfoliated MoS_2 nanosheets were investigated through ultraviolet-visible (UV-Vis) absorption spectroscopy, as reported in Fig. 2. Two peaks appeared at $\lambda \approx 672$ nm and ≈ 612 nm, and can be attributed to the A and B excitons, respectively, corresponding to optical transitions occurring at the K point of the Brillouin zone [16].

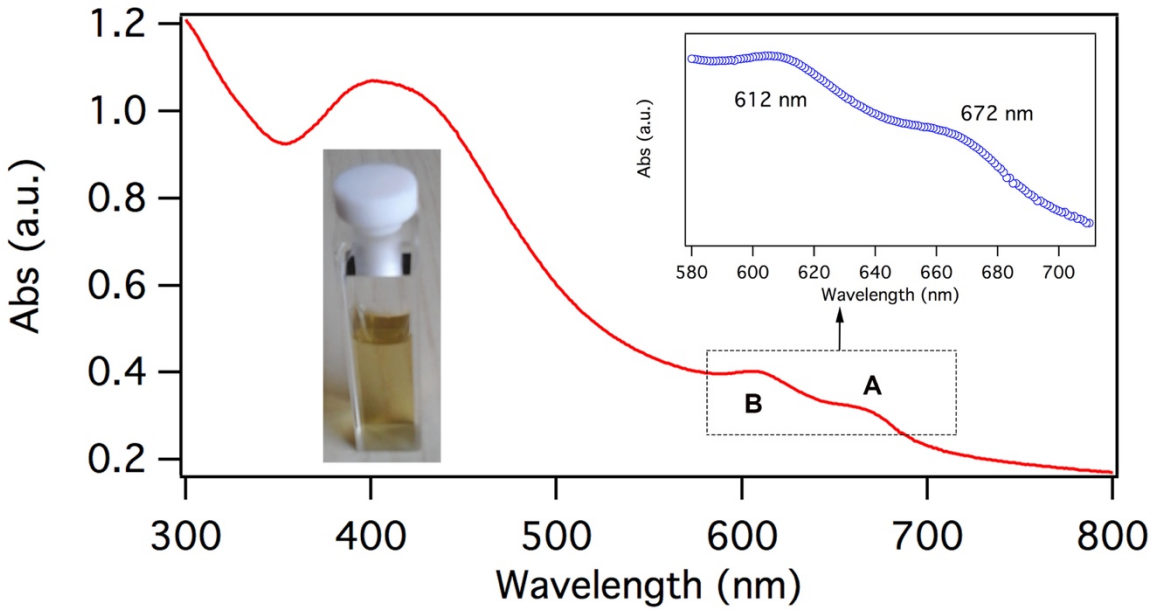

Fig. 2. UV-Vis absorption spectrum of MoS_2 nanosheets dispersed a mixture of H_2O (70%) and ethanol (30%). The inset shows a magnified view of the spectrum in the region of the A and B exciton peaks.

We have performed X-ray photoelectron spectroscopy (XPS) measurements on both pristine and exfoliated material. Fig. 3 compares the Mo 3d and S2p high-resolution XPS spectra of the unexfoliated bulk MoS_2 crystal with those of the nanosheets prepared via lithium-ion intercalation in

DMSO. In the case of pristine MoS_2, the Mo 3d spectrum (Fig. 3a) shows two distinct peaks at 229.4 eV and 232.5 eV, corresponding to the typical Mo^{4+} $3d_{5/2}$ and Mo^{4+} $3d_{3/2}$ spin-orbit components of the semiconducting 2H phase.

The S 2p spectrum displays two peaks at 162.2 eV and 163.4 eV, which are attributed to the S $2p_{3/2}$ and S $2p_{1/2}$ components, respectively (Fig. 3b). On the other hand, in the case of the exfoliated material, the Mo 3d spectrum (Fig. 3c) displays an additional pair of peaks ─ located at lower binding energies ($\Delta E_b \approx 1$ eV) ─ that can be assigned to the metallic 1T phase [38-40]. The S 2p spectrum (Fig. 3d) also presents broader peaks that can be fitted to two pairs of doublets, i.e. those of the 2H phase at high binding energy (green) and those of the 1T phase at low binding energy (light blue). The peak fitting of Mo 3d and S 2p spectra allows estimating the relative content of 1T (~40%) and 2H (~60%) phases (see Fig. S2 and Table S1 in the Supplementary Data).

Our intercalation/exfoliation approach enables the preparation of nanosheets that are preferentially semiconducting, whereas previous works based on chemical or electrochemical methods have shown the formation of metallic nanosheets with 1T content exceeding 60%. The change from 2H to 1T upon intercalation is commonly associated to a strong electron transfer from the lithium atoms to the MoS_2 layers [41, 42]. In our case, the presence of DMSO molecules coordinating the Li ions [37] could presumably mitigate the intercalation step and consequently such electron-transfer process, thereby limiting the conversion to the metallic 1T phase.

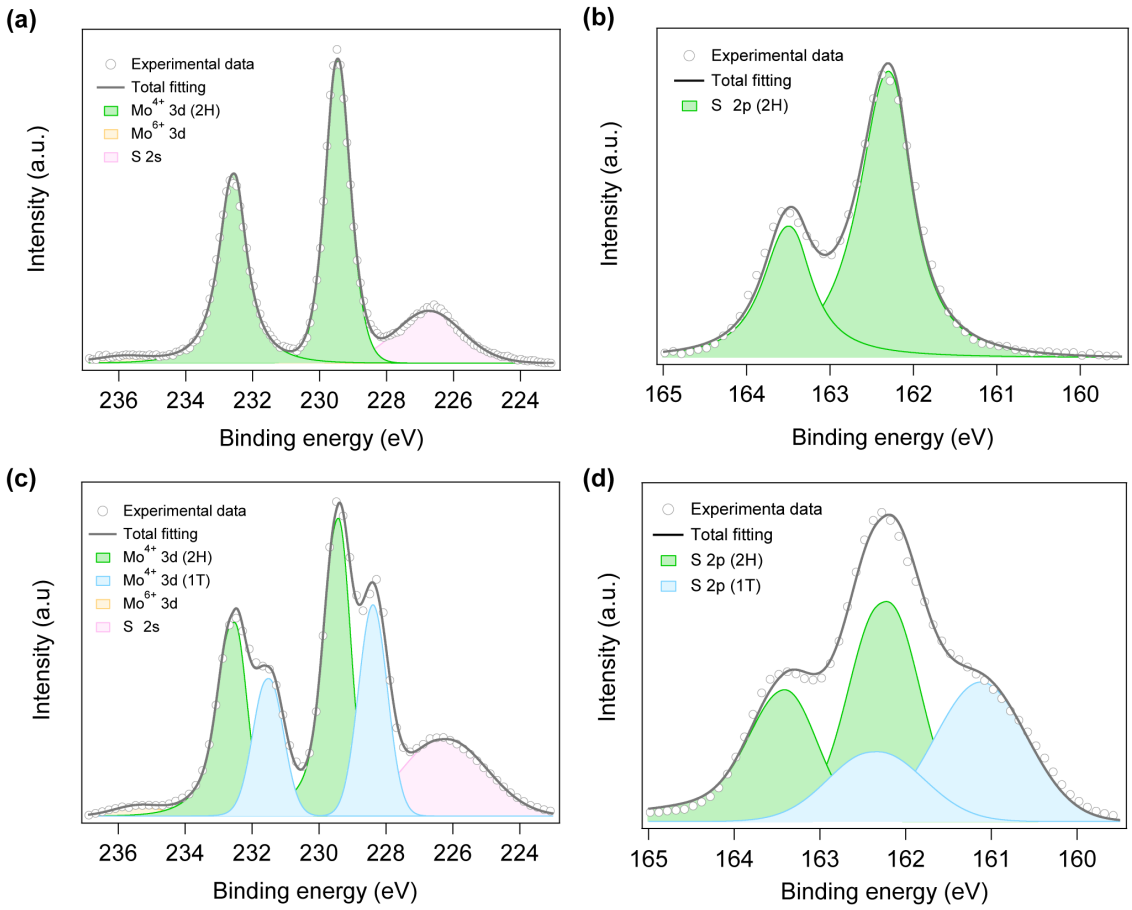

Fig. 3. (a, b) High-resolution XPS spectra of (a) Mo 3d and (b) S 2p regions acquired from unexfoliated MoS_2 crystals. The relatively small peak at 235.7 eV (Mo^{6+} state) reveals the presence of a low level of oxidation in the unexfoliated material. (c, d) High-resolution XPS spectra of the (c) Mo 3d and (d) S 2p regions acquired from MoS_2 nanosheets prepared *via* lithium-ion intercalation in DMSO. The oxidation level is not modified by the intercalation/exfoliation process. All the peak positions were corrected according to the C 1s signal at 284.8 eV.

The structural properties of the exfoliated MoS_2 nanosheets were further investigated by means of Raman spectroscopy, which can provide detailed information on layer thickness [43], atomic coordination, e.g. trigonal prismatic (2H) *vs.* octahedral (1T) [44], as well as on structural disorder [45]. Fig. 4a portrays the Raman spectra of a MoS_2 nanoflake obtained by DMSO-solvated lithium-ion intercalation process (blue) and mechanical exfoliation (red). The former exhibits three additional peaks located at ~157 cm^{-1}, ~227 cm^{-1} and ~331 cm^{-1}, which can be attributed to the J1, J2 and J3 modes of 1T′ crystal phase, respectively. At the same time, the A_{1g} and E^1_{2g} modes maintain a similar frequency and relative intensity ─ see ref. [46] for a comparison between the 1T/1T′ and 2H modes ─ which indicates that both polytypes coexist in our electrochemically intercalated MoS_2 nanosheets

within a lateral scale of ~0.7 μm (laser-beam diameter), in agreement with the results of TEM and XPS investigations. On the other hand, as shown in the Fig. 4b the peaks separation is estimated at ~21.8 cm^{-1} which confirms the formation of an average thickness about two-three monolayers. Noteworthy, the peak at ~227 cm^{-1} can be also ascribed to the longitudinal acoustic phonons (LA) at the M point in the Brillouin that are active only in the presence of defects, as discussed in detail by Mignuzzi and coworkers. The quality of the MoS_2 nanosheets can be assessed by calculating the ratio between the intensities of the LA(M) and A_{1g} modes [21]. If we assume for simplicity that the peak at ~227 cm^{-1} arises exclusively from LA(M) acoustic vibrations, we can extract *I*(LA(M))/*I*(A1g) values within the range 0.1-0.3, which correspond to an average inter-defect distance *L*D of 1-2 nm. The strong contribution of defects in the Raman spectra of electrochemically intercalated MoS_2 can be also evaluated by the line shapes of the A_{1g} and E^1_{2g} modes (Fig. 4b), which are characterized by the presence of shoulder peaks at ~378 cm^{-1} and ~410 cm^{-1}, corresponding to defect-activated LO(M) and ZO(M) phonon modes, respectively. We observed similar line shapes also in the case of defective MoS_2 sheets containing sulfur vacancies with relative density $\Delta S/S \geq 5\%$ generated by low-energy (500 eV) Ar-ion irradiation.

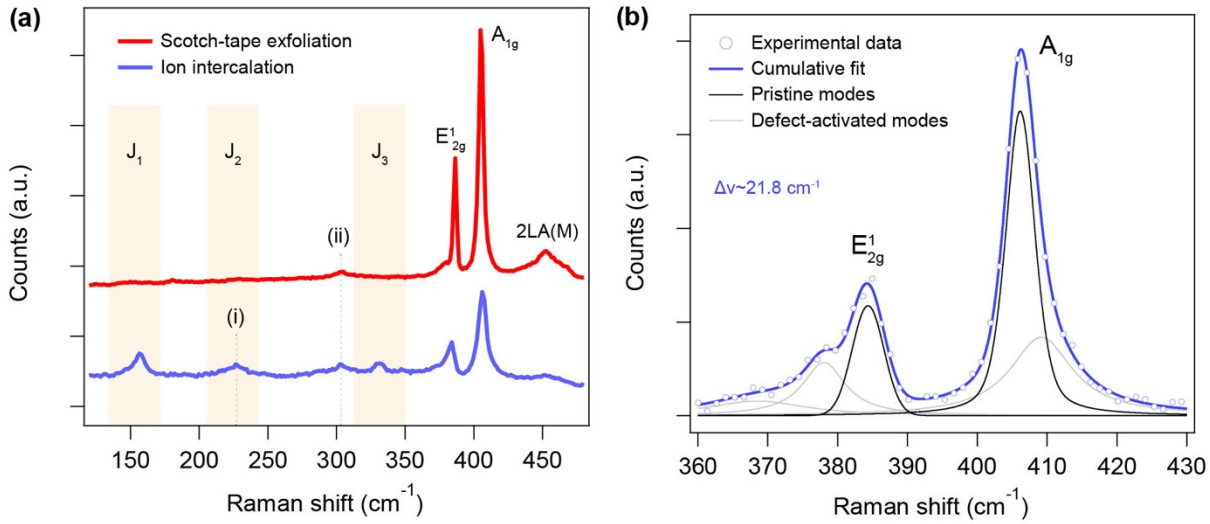

Fig. 4. (a) Raman spectra of MoS_2 nanosheets exfoliated by DMSO-solvated lithium-ion intercalation (blue, bilayer) and scotch-tape technique (red, monolayer). The peak (i) can be also attributed to the defect-activated LA(M) mode at ~227 cm^{-1}, whereas the peak (ii) ─ present in both spectra ─ corresponds to the 2TA(*X*) Raman mode of the SiO_2/Si substrate. (b) Raman spectrum of a bilayer MoS_2 flake obtained *via* DMSO-solvated

lithium-ion intercalation in the spectral region of the E^1_{2g} and A_{1g} modes. The fitting was carried out with the method presented in ref. [45] for defective MoS_2 sheets.

3.3 Field-effect transistors and electrical properties

We investigated the charge-transport properties of individual MoS_2 nanosheets through the fabrication and characterization of back-gated FETs (Fig. 5). As-fabricated devices showed n-type behavior with I_{on}/I_{off} ratios in the range 1-10 and field-effect mobilities μ_{FE} up to 10^{-3} cm^2 V^{-1} s^{-1}. These are several orders of magnitude lower than equivalent devices based on mechanically-exfoliated MoS_2 nanosheets ($\mu_{FE} \approx 30$ cm^2 V^{-1} s^{-1} and $I_{on}/I_{off} \approx 10^7$), likely due to a high degree of disorder associated to the 2H/1T nanoscale polymorphism ─ confirmed by multiple experimental techniques (i.e. HR-TEM, XPS and Raman spectroscopy) ─ and defects generated during the intercalation/exfoliation process.

Following common procedures reported in literature for Au-contacted MoS_2 FETs, we have carried out a high-vacuum annealing step at 150 °C for about 15 hours (base pressure ~ 5×10^{-8} mbar) in order to reduce the contact resistance, as well to remove solvent traces and environmental adsorbates [47]. On average, such a process leads to an increase of μ_{FE} by approximatively one order of magnitude, but does not improve significantly the I_{on}/I_{off} ratio.

Typical output and transfer characteristics acquired under inert atmosphere (N_2-filled glovebox) are reported in the supplementary data (Fig. S3). It should be noticed that thermal annealing at 150°C can also induce a partial back-conversion of the 1T phase into 2H, as revealed by Raman studies conducted on MoS_2 nanosheets vacuum-annealed at different temperatures. Unexpectedly, annealing at higher temperatures (~250 °C), which was supposed to be beneficial for the complete 1T-to-2H conversion (Fig. S4), led to a significant drop in in field-effect mobility ($\mu_{FE} \leq 10^{-4}$ cm^2 V^{-1} s^{-1}).

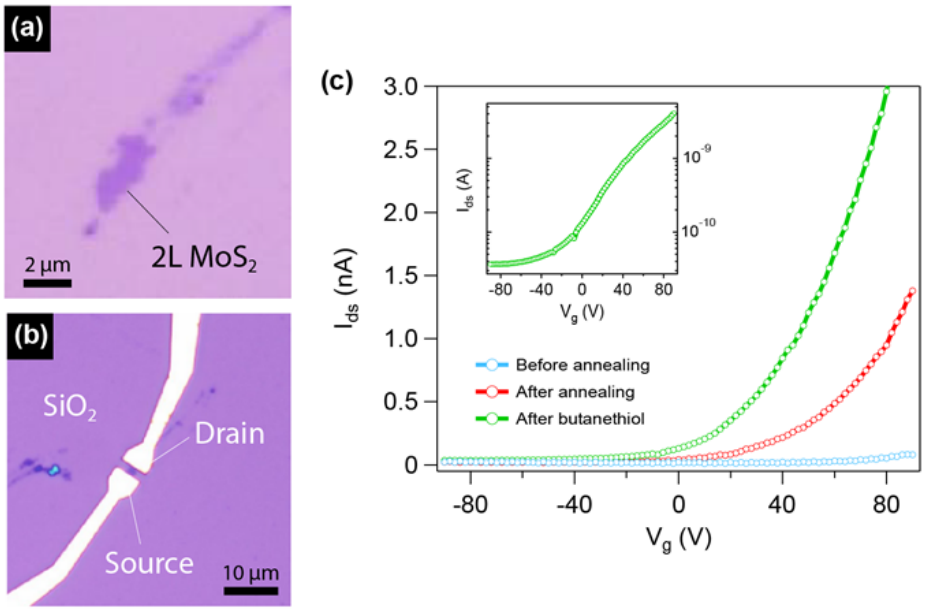

Fig. 5. Fabrication and characterization of FETs based on exfoliated MoS_2 nanosheets. (a,b) Optical micrographs of a bilayer MoS_2 flake deposited on a SiO_2/Si substrate before (a) and after (b) the fabrication of the source and drain contacts (Au, 90 nm). The heavily-doped silicon substrate is used as the back gate. (c) Transfer curves of the FET device shown in (b) acquired at different stages under inert atmosphere (N_2-filled glovebox). The drain-source bias voltage V_{ds} was set at 4 V. The curve obtained after butanethiol treatment (green) is reported in semi-log scale in the inset and displays I_{on}/I_{off} current ratio up to 10^2.

We expect that such degradation ─ not observed in the case of mechanically exfoliated MoS_2 sheets (see supplementary data, Section 5) ─ stems from the thermal evolution/expansion of defects, which involves the formation of grain boundaries following to the rearrangements of 1T domains into 2H domains. At this stage, more comprehensive studies are needed to shed light on the effects of the exfoliation-induced disorder on the charge-transport properties of MoS_2 nanosheets, which is however beyond the scope of the present work.

Finally, we noticed that sulfur vacancies could be generated during ion intercalation and exfoliation. Indeed, X-ray photoemission spectroscopy (XPS) measurements revealed that the exfoliation process leads to a reduction of the S/Mo stoichiometric ratio, from ~2 for the bulk form to ~1.94 for the exfoliated nanosheets (see Section 3 in supplementary data). Hence, we explored the use of a vapor-phase chemical treatment with butanethiols molecules, with the aim of improving the electrical characteristics of our FETs by vacancy healing. Fig. 5b shows the effect of the butanethiol treatment on the transfer characteristics of a device fabricated on a bilayer MoS_2 nanosheet. Upon exposure to

butanethiol molecules, the field-effect mobility μ_{FE} improves by a more than a factor 3 and the I_{on}/I_{off} current ratio reaches ~10^2 (inset). Such a remarkable improvement suggests that sulfur vacancies are abundant defects in our chemically-exfoliated nanosheets. By and large, it should be noticed that the figures of merit of our devices are comparable with those reported in the literature for liquid-phase exfoliated nanosheets and their network films [21, 48, 49]; however, they remain still much lower than those of mechanically-exfoliated MoS_2 flakes [10, 47, 50-52], indicating that other forms of disorder ─ as discussed above ─ are responsible for the degradation of the charge-transport properties in the nanosheets obtained via lithium-ion intercalation in DMSO.

4. Conclusions

In summary, we have presented a facile, fast and low-cost approach to exfoliate MoS_2 crystals under ambient conditions via DMSO-solvated lithium-ion intercalation. Our method allows producing single-, bi- and tri-layer thick nanosheets of MoS_2 with an average lateral size of ~0.8 μm. HR-TEM, XPS and Raman spectroscopy revealed the presence of a large amount of semiconducting 2H phase (~60%). The electronic properties of the nanoflakes were investigated through the fabrication and characterization of back-gated field-effect transistors (FETs), which displayed unipolar semiconducting behavior (*n*-type), in line with the observation of a predominant 2H phase within the exfoliated flakes. We succeeded in improving the electronic properties of our FETs through a combination of vacuum annealing and defect healing with short linear thiolated molecules, resulting in μFE values up to 2×10^{-2} cm^2 V^{-1} s^{-1} and $I_{on}/I_{off} \approx 100$. Our results on vacuum annealing of MoS_2 nanosheets with mixed 1T/2H phases cast the basis for future investigations on the influence of exfoliation-induced disorder on the charge transport properties. The approach presented in this work paves the ways towards the fast preparation ─ under ambient conditions ─ of semiconducting MoS_2 nanosheets, which can be conveniently employed in low-cost flexible (opto-) electronic devices.

Author contributions

‡ These authors equally contributed to this work

Acknowledgements

Device fabrication was carried out in part at the nanotechnology facility STNano (IPCMS) with the assistance of S. Siegwald. We acknowledge financial support from the European Commission through the Graphene Flagship Core 2 project (GA-785219) and the Marie-Curie IEF MULTI2DSWITCH (GA-700802), the IRTG Soft Matter Science, the Agence Nationale de la Recherche through the LabEx project Nanostructures in Interaction with their Environment (ANR-11-LABX-0058_NIE), the International Center for Frontier Research in Chemistry (icFRC), and the Polish National Science Center (Grant. No. 2015/18/E/ST5/00188).

References

[1] K.S. Novoselov, A.K. Geim, S.V. Morozov, D. Jiang, Y. Zhang, S.V. Dubonos, I.V. Grigorieva, A.A. Firsov, Electric field effect in atomically thin carbon films, Science 306 (2004) 666-669.

[2] A.K. Geim, K.S. Novoselov, The rise of graphene, Nat. Mater. 6 (2007) 183-191.

[3] M. Chhowalla, H.S. Shin, G. Eda, L.-J. Li, K.P. Loh, H. Zhang, The chemistry of two-dimensional layered transition metal dichalcogenide nanosheets, Nat. Chem. 5 (2013) 263-275.

[4] M. Xu, T. Liang, M. Shi, H. Chen, Graphene-like two-dimensional materials, Chem. Rev. 113 (2013) 3766-3798.

[5] G.R. Bhimanapati, Z. Lin, V. Meunier, Y. Jung, J. Cha, S. Das, D. Xiao, Y. Son, M.S. Strano, V.R. Cooper, Recent advances in two-dimensional materials beyond graphene, ACS Nano 9 (2015) 11509-11539.

[6] X. Cao, C. Tan, X. Zhang, W. Zhao, H. Zhang, Solution-processed two-dimensional metal dichalcogenide-based nanomaterials for energy storage and conversion, Adv. Mater. 28 (2016) 6167-6196.

[7] Z. He, W. Que, Molybdenum disulfide nanomaterials: structures, properties, synthesis and recent progress on hydrogen evolution reaction, Appl. Mater. Today 3 (2016) 23-56.

[8] J. Zhang, T. Wang, D. Pohl, B. Rellinghaus, R. Dong, S. Liu, X. Zhuang, X. Feng, Interface engineering of MoS_2/Ni_3S_2 heterostructures for highly enhanced electrochemical overall-water-splitting activity, Angew. Chem. Int. Ed. 128 (2016) 6814-6819.

[9] G. Fiori, F. Bonaccorso, G. Iannaccone, T. Palacios, D. Neumaier, A. Seabaugh, S.K. Banerjee, L. Colombo, Electronics based on two-dimensional materials, Nat. Nanotechnol. 9 (2014) 768-779.

[10] R. {Radisavljevic, B., A. Radenovic, J. Brivio, V. Giacometti, A. Kis, Single-layer MoS_2 transistors, Nat. Nanotechnol. 6 (2011) 147-150.

[11] Q.H. Wang, K. Kalantar-Zadeh, A. Kis, J.N. Coleman, M.S. Strano, Electronics and optoelectronics of two-dimensional transition metal dichalcogenides, Nat. Nanotechnol. 7 (2012) 699-712.

[12] Y. Huang, J. Guo, Y. Kang, Y. Ai, C.M. Li, Two dimensional atomically thin MoS_2 nanosheets and their sensing applications, Nanoscale 7 (2015) 19358-19376.

[13] M. Pumera, A.H. Loo, Layered transition-metal dichalcogenides (MoS_2 and WS_2) for sensing and biosensing, Trends Anal. Chem. 61 (2014) 49-53.

[14] K.S. Novoselov, D. Jiang, F. Schedin, T.J. Booth, V.V. Khotkevich, S.V. Morozov, A.K. Geim, Two-dimensional atomic crystals, Proc. Natl. Acad. Sci. U.S.A. 102 (2005) 10451-10453.

[15] A. Ciesielski, P. Samorì, Graphene via sonication assisted liquid-phase exfoliation, Chem. Soc. Rev. 43 (2014) 381-398.

[16] G. Eda, H. Yamaguchi, D. Voiry, T. Fujita, M. Chen, M. Chhowalla, Photoluminescence from chemically exfoliated MoS_2, Nano Lett. 11 (2011) 5111-5116.

[17] J.N. Coleman, M. Lotya, A. O'Neill, S.D. Bergin, P.J. King, U. Khan, K. Young, A. Gaucher, S. De, R.J. Smith, Two-dimensional nanosheets produced by liquid exfoliation of layered materials, Science 331 (2011) 568-571.

[18] X. Fan, P. Xu, D. Zhou, Y. Sun, Y.C. Li, M.A.T. Nguyen, M. Terrones, T.E. Mallouk, Fast and efficient preparation of exfoliated 2H MoS_2 nanosheets by sonication-assisted lithium intercalation and infrared laser-induced 1T to 2H phase reversion, Nano Lett. 15 (2015) 5956-5960.

[19] Y. Qi, N. Wang, Q. Xu, H. Li, P. Zhou, X. Lu, G. Zhao, A green route to fabricate MoS_2 nanosheets in water–ethanol–CO_2, Chem. Commun. 51 (2015) 6726-6729.

[20] N. Liu, P. Kim, J.H. Kim, J.H. Ye, S. Kim, C.J. Lee, Large-area atomically thin MoS_2 nanosheets prepared using electrochemical exfoliation, ACS Nano 8 (2014) 6902-6910.

[21] Z. Zeng, Z. Yin, X. Huang, H. Li, Q. He, G. Lu, F. Boey, H. Zhang, Single-layer semiconducting nanosheets: high-yield preparation and device fabrication, Angew. Chem. Int. Ed. 50 (2011) 11093-11097.

[22] X. You, N. Liu, C.J. Lee, J.J. Pak, An electrochemical route to MoS_2 nanosheets for device applications, Mater. Lett. 121 (2014) 31-35.

[23] A.M. Abdelkader, A.J. Cooper, R.A.W. Dryfe, I.A. Kinloch, How to get between the sheets: a review of recent works on the electrochemical exfoliation of graphene materials from bulk graphite, Nanoscale 7 (2015) 6944-6956.

[24] M. Chhowalla, G.A.J. Amaratunga, Thin films of fullerene-like MoS_2 nanoparticles with ultra-low friction and wear, Nature 407 (2000) 164-167.

[25] P.D. Fleischauer, R. Bauer, Chemical and structural effects on the lubrication properties of sputtered MoS_2 films, Tribol. Trans. 31 (1988) 239-250.

[26] D. Yang, S.J. Sandoval, W.M.R. Divigalpitiya, J.C. Irwin, R.F. Frindt, Structure of single-molecular-layer MoS_2, Phys. Rev. B 43 (1991) 12053-12056.

[27] M. Acerce, D. Voiry, M. Chhowalla, Metallic 1T phase MoS_2 nanosheets as supercapacitor electrode materials, Nat. Nanotechnol. 10 (2015) 313-318.

[28] J. Kim, J.S. Kim, T. Kim, H. Choi, J. Lee, H.J. Ji, S.C. Lim, Phase conversion of chemically exfoliated molybdenum disulfide, Curr. Appl. Phys. 17 (2017) 60-65.

[29] D.Y. Xu, Y.Z. Zhu, J.P. Liu, Y. Li, W.C. Peng, G.L. Zhang, F.B. Zhang, X.B. Fan, Microwave-assisted 1T to 2H phase reversion of MoS_2 in solution: a fast route to processable dispersions of 2H-MoS_2 nanosheets and nanocomposites, Nanotechnology 27 (2016) 385604.

[30] A. Ejigu, I.A. Kinloch, E. Prestat, R.A.W. Dryfe, A simple electrochemical route to metallic phase trilayer MoS_2: evaluation as electrocatalysts and supercapacitors, J. Mater. Chem. A 5 (2017) 11316-11330.

[31] E.L.K. Chng, Z. Sofer, M. Pumera, MoS_2 exhibits stronger toxicity with increased exfoliation, Nanoscale 6 (2014) 14412-14418.

[32] M.A. Lukowski, A.S. Daniel, F. Meng, A. Forticaux, L. Li, S. Jin, Enhanced hydrogen evolution catalysis from chemically exfoliated metallic MoS_2 nanosheets, J. Am. Chem. Soc. 135 (2013) 10274-10277.

[33] A. Ambrosi, Z. Sofer, M. Pumera, Lithium intercalation compound dramatically influences the electrochemical properties of exfoliated MoS_2, Small 11 (2015) 605-612.

[34] S. Bertolazzi, S. Bonacchi, G. Nan, A. Pershin, D. Beljonne, P. Samorì, Engineering chemically active defects in monolayer MoS_2 transistors via ion-beam irradiation and their healing via vapor deposition of alkanethiols, Adv. Mater. 29 (2017) 1606760.

[35] A. Ejigu, B. Miller, I.A. Kinloch, R.A.W. Dryfe, Optimisation of electrolytic solvents for simultaneous electrochemical exfoliation and functionalisation of graphene with metal nanostructures, Carbon 128 (2018) 257-266.

[36] X.-R. Liu, L. Wang, L.-J. Wan, D. Wang, In situ observation of electrolyte-concentration-dependent solid electrolyte interphase on graphite in dimethyl sulfoxide, ACS Appl. Mater. Interfaces 7 (2015) 9573-9580.

[37] E. Westphal, J.R. Pliego Jr, Absolute solvation free energy of Li^+ and Na^+ ions in dimethyl sulfoxide solution: a theoretical ab initio and cluster-continuum model study, J. Chem. Phys. 123 (2005) 074508.

[38] L. Jiang, S. Zhang, S.A. Kulinich, X. Song, J. Zhu, X. Wang, H. Zeng, Optimizing hybridization of 1T and 2H phases in MoS_2 monolayers to improve capacitances of supercapacitors, Mater. Res. Lett. 3 (2015) 177-183.

[39] D.R. Cummins, U. Martinez, A. Sherehiy, R. Kappera, A. Martinez-Garcia, R.K. Schulze, J. Jasinski, J. Zhang, R.K. Gupta, J. Lou, Efficient hydrogen evolution in transition metal dichalcogenides via a simple one-step hydrazine reaction, Nat. Commun. 7 (2016) 11857.

[40] K.C. Knirsch, N.C. Berner, H.C. Nerl, C.S. Cucinotta, Z. Gholamvand, N. McEvoy, Z. Wang, I. Abramovic, P. Vecera, M. Halik, Basal-plane functionalization of chemically exfoliated molybdenum disulfide by diazonium salts, ACS Nano 9 (2015) 6018-6030.

[41] C.A. Papageorgopoulos, W. Jaegermann, Li intercalation across and along the van der Waals surfaces of MoS_2 (0001), Surf. Sci. 338 (1995) 83-93.

[42] D. Voiry, A. Mohite, M. Chhowalla, Phase engineering of transition metal dichalcogenides, Chem. Soc. Rev. 44 (2015) 2702-2712.

[43] C. Lee, H. Yan, L.E. Brus, T.F. Heinz, J. Hone, S. Ryu, Anomalous lattice vibrations of single- and few-layer MoS_2, ACS Nano 4 (2010) 2695-2700.

[44] S.J. Sandoval, D. Yang, R.F. Frindt, J.C. Irwin, Raman study and lattice dynamics of single molecular layers of MoS_2, Phys. Rev. B 44 (1991) 3955-3962.

[45] S. Mignuzzi, A.J. Pollard, N. Bonini, B. Brennan, I.S. Gilmore, M.A. Pimenta, D. Richards, D. Roy, Effect of disorder on Raman scattering of single-layer MoS_2, Phys. Rev. B 91 (2015) 195411.

[46] M. Calandra, Chemically exfoliated single-layer MoS_2: stability, lattice dynamics, and catalytic adsorption from first principles, Phys. Rev. B 88 (2013) 245428.

[47] S.L. Li, K. Tsukagoshi, E. Orgiu, P. Samorì, Charge transport and mobility engineering in two-dimensional transition metal chalcogenide semiconductors, Chem. Soc. Rev. 45 (2016) 118-151.

[48] A.G. Kelly, T. Hallam, C. Backes, A. Harvey, A.S. Esmaeily, I. Godwin, J. Coelho, V. Nicolosi, J. Lauth, A. Kulkarni, S. Kinge, L.D.A. Siebbeles, G.S. Duesberg, J.N. Coleman, All-printed thin-film transistors from networks of liquid-exfoliated nanosheets, Science 356 (2017) 69-72.

[49] K.C. Knirsch, N.C. Berner, H.C. Nerl, C.S. Cucinotta, Z. Gholamvand, N. McEvoy, Z.X. Wang, I. Abramovic, P. Vecera, M. Halik, S. Sanvito, G.S. Duesberg, V. Nicolosi, F. Hauke, A. Hirsch, J.N. Colernan, C. Backes, Basal-plane functionalization of chemically exfoliated molybdenum disulfide by diazonium salts, ACS Nano 9 (2015) 6018-6030.

[50] B. Radisavljevic, A. Kis, Measurement of mobility in dual-gated MoS_2 transistors, Nat. Nanotechnol. 8 (2013) 147-148.

[51] B. Radisavljevic, A. Kis, Mobility engineering and a metal-insulator transition in monolayer MoS_2, Nature Materials 12 (2013) 815-820.

[52] M.S. Fuhrer, J. Hone, Measurement of mobility in dual-gated MoS_2 transistors, Nature Nanotechnology 8 (2013) 146.